Aryloxide and Alkoxide Derivatives of Metal Clusters. Syntheses, Structures, and Reactivities of the μ-Oxo-Bridged Triruthenium Clusters $Ru_3(CO)_8(\mu\text{-}\eta^2\text{-}OC_6H_4Cl)_2$ and $Ru_3(CO)_8(\mu\text{-}\eta^2\text{-}OCH_2C_5H_4N)_2$

Donald J. Darensbourg,*[1a] Bernardo Fontal,*[1b] Steve S. Chojnacki,[1a] Kevin K. Klausmeyer,[1a] and Joseph H. Reibenspies[1a]

Departments of Chemistry, Texas A&M University, College Station, Texas 77843, and Universidad de Los Andes, Merida, Venezuela

Received December 22, 1993[⊗]

The halide-stabilized phenol derivatives of triruthenium carbonyl $Ru_3(CO)_8(\mu\text{-}\eta^2\text{-}OC_6H_4X)_2$ (X = F, Cl, Br) have been synthesized via the reaction of $Ru_3(CO)_{12}$ with the corresponding phenol (o-XC_6H_4OH) and anhydrous Me_3NO. The complex where X = Cl (**1**) has been characterized both in solution by FTIR and $^1H/^{13}C$ NMR spectroscopies and in the solid-state by X-ray crystallography. The o-$OC_6H_4Cl^-$ ligands serve as five-electron donor groups which bridge an edge of the triruthenium framework, with the bridged Ru···Ru separation being significantly longer (3.042(1) Å) than the other two Ru–Ru bond distances, which average 2.738[1] Å. The coordination spheres of the ruthenium centers, which are μ-oxygen atom bridged, are completed by interactions with the chloride substituents on the phenol ligands. The unique ruthenium atom has a $Ru(CO)_4$ structure similar to that of the parent dodecacarbonyl cluster. Complex **1** is shown to reversibly react with carbon monoxide to disrupt the Ru···Cl interaction to afford unstable $Ru_3(CO)_{8+n}(\mu\text{-}OC_6H_4Cl)_2$ (n = 1, 2) species. Similarly, complex **1** reacts sequentially with a variety of donor ligands (L) to provide more stable $Ru_3(CO)_8L_2(\mu\text{-}OC_6H_4X)_2$ derivatives. A stable prototype of one such complex, $Ru_3(CO)_8(\mu\text{-}\eta^2\text{-}OCH_2C_5H_4N)_2$ (**12**), was prepared from $Ru_3(CO)_{12}$ and pyridinecarbinol in the presence of anhydrous Me_3NO. This derivative was characterized in the solid state by X-ray crystallography. It was shown to possess two ruthenium metal centers (nonbonded at 3.024(1) Å) bridged by two alkoxide μ-O atoms, with each pyridine substituent further being bonded to a ruthenium atom. The bonded Ru–Ru distances in the triangular cluster averaged 2.783[1] Å. Crystal data for **1**: orthorhombic space group *Pbca*, a = 18.676(4) Å, b = 9.106(2) Å, c = 28.496(6) Å, Z = 8, R = 5.07%. Crystal data for **12**: space group $P2_1/c$, a = 12.305(3) Å, b = 10.331(2) Å, c = 18.489(4) Å, β = 90.67(2)°, Z = 4, R = 3.08%.

Introduction

The delineation of surface intermediates derived from the interaction of ruthenium carbonyl clusters with metal oxides supports is often quite difficult, as compared with the delineation of surface intermediates in analogous processes involving osmium clusters, because of the more reactive nature of ruthenium carbonyl.[2] Consequently, an adequate description of the corresponding surface organometallic chemistry is generally lacking. This situation can be somewhat ameliorated by the synthesis and characterization of good model complexes. An example of such a surface interaction is provided in eq 1, which depicts the proposed

$$Ru_3(CO)_{12} + HOSi\equiv \longrightarrow HRu_3(CO)_{10}OSi\equiv + 2CO \qquad (1)$$

stoichiometry of the surface reaction between the triangular ruthenium or osmium clusters and silica.[3] In general, there are several examples of metallic clusters containing oxygen donor ligands.[4] Although phenol derivatives of osmium[5] and carboxylates of ruthenium[6] have been reported for some time, only recently have there been reports of phenol derivatives of ruthenium.[7,8]

We report herein the synthesis, reactivity in solution, solid-state and solution characterization of an aryloxide ruthenium cluster stabilized by chloride interaction, $Ru_3(CO)_8(\mu\text{-}\eta^2\text{-}OC_6H_4Cl)_2$ (**1**), a derivative which is a representative model for the interaction of $Ru_3(CO)_{12}$ with metal oxides. In addition, the solid-state structure of $Ru_3(CO)_8(\mu\text{-}\eta^2\text{-}OCH_2C_5H_4N)_2$, a species prototypical of the derivative formed from the reaction of **1** with pyridine, is described.

Experimental Section

All manipulations were carried out on a double-manifold Schlenk vacuum line under a dry nitrogen atmosphere. The solvents, methylene chloride and hexane, were dried under nitrogen by distillation from phosphorus pentoxide and sodium benzophenone ketyl, respectively. $Ru_3(CO)_{12}$ was purchased from Strem Chemicals and used directly. Trimethylamine oxide (Aldrich Chemical Co.) was dried by heating to sublimation at 80 °C under vacuum, a process repeated at least three times in order to obtain pure oxide. Infrared spectra were recorded on an IBM FTIR 32 spectrometer. Proton, ^{31}P, and ^{13}C NMR spectra were determined on a Varian XL-200 spectrometer. Microanalyses were performed by Galbraith Laboratories, Inc., Knoxville, TN.

Synthesis of $Ru_3(CO)_8(\mu\text{-}\eta^2\text{-}OC_6H_4Cl)_2$ (1). In a typical reaction, a solution of $Ru_3(CO)_{12}$ (0.20 g, 0.32 mmol) in 70 mL of dried/deoxygenated

⊗ Abstract published in *Advance ACS Abstracts*, July 1, 1994.

(1) (a) Texas A&M University. (b) Universidad de Los Andes.

(2) Lavigne, G. In *The Chemistry of Metal Cluster Complexes*; Shriver, D. F., Kaesz, H. D., Adams, R. D., Eds.; VCH Publishers: New York, 1990; p 201 and references therein.

(3) (a) D'Ornelas, L.; Choplin, A.; Basset, J. M.; Hsu, L. Y.; Shore, S. G. *Nouv. J. Chim.* **1985**, *9*, 155. (b) Psaro, R.; Ugo, R. In *Metal Clusters in Catalysis*; Gates, B. C., Guczi, L., Knözinger, H., Eds.; Elsevier: Amsterdam, 1986; p 427 and references therein. (c) Puga, J.; Fehlner, T. P.; Gates, B. C.; Braga, D.; Grepioni, F. *Inorg. Chem.* **1990**, *29*, 2376.

(4) Azam, K. A.; Deeming, A. J.; Kimber, R. E.; Shukla, P. R. *J. Chem. Soc., Dalton Trans.* **1976**, 1853.

(5) Choplin, A.; Besson, B.; D'Ornelas, L.; Sanchez-Delgado, R.; Basset, J. M. *J. Am. Chem. Soc.* **1988**, *110*, 2783.

(6) (a) Darensbourg, D. J.; Gray, R. L.; Pala, M. *Organometallics* **1984**, *3*, 1928. (b) Anstock, M.; Taube, D.; Gross, D. C.; Ford, P. C. *J. Am. Chem. Soc.* **1984**, *106*, 3696. (c) Darensbourg, D. J.; Pala, M.; Waller, J. *Organometallics* **1983**, *2*, 1285. (d) Taube, D.; Rokicki, A.; Ford, P. C. *Inorg. Chem.* **1987**, *26*, 526.

(7) Santini, C. C.; Basset, J. M.; Fontal, B.; Krause, J.; Shore, S. G.; Charrier, C. *J. Chem. Soc., Chem. Commun.* **1987**, 512.

(8) Bohle, D. S.; Vahrenkamp, H. *Angew. Chem., Int. Ed. Engl.* **1990**, *29*, 198.

0020-1669/94/1333-3526$04.50/0

CH_2Cl_2 was cooled to −78 °C. An anhydrous solution of $(CH_3)_3NO$ (0.072 g, 0.96 mmol) in 15 mL of CH_2Cl_2 was slowly added to the $Ru_3(CO)_{12}$ under vigorous nitrogen bubbling in order to remove carbon monoxide and trimethylamine, subsequent to the addition of a methylene chloride solution of o-ClC_6H_4OH (0.05 mL, 0.80 mmol). The reaction solution was allowed to warm to ambient temperature and heated to 50 °C for 45 min under a purge of nitrogen. Finally the solution was evaporated to dryness under vacuum and extracted with hot hexane, the extract was filtered, and the filtrate was reduced in volume to about 30 mL. Upon cooling of the solution, a 40% yield (0.10 g) of $Ru_3(CO)_8(\mu\text{-}\eta^2\text{-}OC_6H_4Cl)_2$ (**1**) was obtained as brown needles. The infrared ν(CO) spectrum in hexane displayed bands at 2111 (w), 2044 (s), 2027 (vs), 2001 (vw), and 1953 (m) cm^{-1}. The ^1H NMR spectrum in $CDCl_3$ of the o-$OC_6H_4Cl^-$ ligand in **1** exhibited an ABCD pattern with the following values:[9a] δ 7.10 [$J(H_AH_B)$ = 8.22, $J(H_AH_C)$ = 1.9, $J(H_AH_D)$ = 0.0 Hz; H_A], 7.17 [$J(H_BH_C)$ = 6.78, $J(H_BH_D)$ = 1.42 Hz; H_B], 6.68 [$J(H_CH_D)$ = 8.16 Hz; H_C], 7.03 [H_D]. ^{13}C NMR ($CDCl_3$) (room temperature, natural abundance):[9b] δ(o-OC_6H_4Cl ligand) 159.9 (C-1), 119.4 (C-2), 126.2 (C-3), 122.1 (C-4), 127.9 (C-5), 119.4 (C-6); δ(Ru–CO) 197.4, 184.4. Anal. Calc for $Ru_3Cl_2O_{10}C_{20}H_8$: C, 30.68; H, 1.02; Cl, 9.07. Found: C, 30.32; H, 0.75; Cl, 9.45. A highly ^{13}CO-enriched sample of **1**, $Ru_3(^{13}CO)_8(\mu\text{-}\eta^2\text{-}OC_6H_4Cl)_2$ (**1a**), was prepared from $Ru_3(^{13}CO)_{12}$ (prepared as previously described[6a]) in an otherwise completely analogous manner. IR (hexane): ν(CO) 2060 (w), 1999 (vs), 1980 (s), 1959 (vw), 1908 (m) cm^{-1}.

Preparation of Other $Ru_3(CO)_8(\mu\text{-}\eta^2\text{-}OC_6H_4X)_2$ Derivatives (X = F, Br) and $Ru_3(CO)_8(\mu\text{-}\eta^2\text{-}OC_6H_3Cl_2)$. Complexes analogous to complex **1** were prepared in lower yields by a similar procedure with somewhat longer reaction times. For X = F (**2**), the complex is obtained as a red-brown solid with ν(CO) vibrations in hexane at 2106 (w), 2036 (s), 2020 (vs), 1992 (vw), and 1941 (m) cm^{-1}. In a like manner when X = Br (**3**), the complex is orange with an infrared spectrum in the ν(CO) region in hexane: 2107 (w), 2041 (s), 2026 (vs), 2000 (vw), 1952 (m) cm^{-1}. The $Ru_3(CO)_8(\mu\text{-}\eta^2\text{-}OC_6H_3Cl_2)$ (**4**) complex was obtained as an orange-brown solid with IR (hexane) ν(CO) at 2112 (w), 2047 (s), 2030 (vs), 2002 (vw), and 1957 (m) cm^{-1}.

Reactivity Studies of $Ru_3(CO)_8(\mu\text{-}\eta^2\text{-}OC_6H_4Cl)_2$ with Lewis Bases. Carbon Monoxide. CO (or ^{13}CO, 1 atm static) was bubbled through a hexane solution of **1** (or **1a**) at ambient temperature for 1 h (or 20 min at 50 °C). The reaction was reversed by slowly bubbling nitrogen through the solution at 50 °C for 30 min. The infrared ν(CO) spectra in hexane were as follows: ^{12}CO saturated on **1**, 2111 (w), 2077 (m, br), 2066 (w), 2044 (vw), 2033 (vs), 2027 (vw), 2018 (vw), 2002 (vw), 1995 (vw), 1952 (w) cm^{-1}; ^{13}CO saturated on **1**, 2108 (w), 2097 (w), 2044 (vs), 2018 (s), 1963 (m), 1909 (s) cm^{-1}. The latter spectrum reverts to that of the ^{12}C species upon addition of ^{12}CO.

Pyridine. Pyridine dissolved in hexane (1:20) was added dropwise to a hexane solution of **1** (0.01 g/15 mL), during which time a red-brown color developed and a red-brown flaky precipitate formed (**5**). Upon further addition of pyridine, the precipitate redissolved to provide a yellow solution. Light yellow-beige needles formed upon cooling the solution (**6**). Both compounds were thermally stable and unreactive toward CO at ambient temperature. IR (hexane), ν(CO) **5**, 2102 (mw), 2038 (vw), 2032 (s), 2020 (vs), 1992 (w), 1944 (m) cm^{-1}; **6**, 2093 (mw), 2032 (m), 2017 (vs), 2010 (m), 2002 (vw), 1940 (m) cm^{-1}. ^1H NMR in $CDCl_3$: **5**, δ(bound pyridine) 8.40 (br), 7.56 (br), 7.07 (br); δ(bound $-OC_6H_4Cl$) multiplet between 7.33 and 6.38 ppm. Relative pyridine:phenol ligand integrated intensity: ca. 5:7. **6**: δ(bound pyridine) 8.49 (br), 7.68 (br), 7.20 (br); δ(bound $-OC_6H_4Cl$) multiplet between 7.38 and 6.38 ppm. Relative pyridine:phenol integrated intensity: ligand: ca. 10:7. Anal. Calc for $Ru_3N_2O_{10}Cl_2C_{30}H_{18}$ (**6**): C, 38.28; H, 1.91; N, 2.97; Cl, 7.55. Found: C, 39.47; H, 1.67; N, 3.22; Cl, 5.07.

Triphenylphosphine. Triphenylphosphine dissolved in hexane was added to a hexane solution of **1**. A red-orange color developed rapidly, resulting in a complex which was thermally stable at 50 °C and unreactive toward carbon monoxide. IR (hexane): ν(CO) 2096 (ms), 2035 (mw), 2027 (vs), 2020 (vs), 2007 (vw), 1949 (w), 1941 (mw) cm^{-1}. On further addition of PPh_3 and longer reaction time, an orange solid forms (**7**). IR (CH_2Cl_2): ν(CO) 2058 (s, br), 2007 (vs), 1987 (m, br), 1965 (m, br), 1939 (w, br), 1607 (vs) cm^{-1}. Upon addition of CO, no change in the infrared ν(CO) spectrum resulted. Exactly the same complex results from the reaction of $Ru_3(CO)_8(\mu\text{-}\eta^2\text{-}OC_6H_4OMe)_2$[7] with triphenylphosphine. ^1H NMR ($CDCl_3$) of **7**: δ(bound PPh_3) multiplet between 7.40 and 7.13 ppm. ^{31}P NMR ($CDCl_3$) of **7**: δ 17.9 (s). Anal. Calc for $Ru_3P_2O_{10}C_{46}H_{28}$ (**7**): C, 49.9; H, 2.53; P, 5.60. Found: C, 48.23; H, 2.72; P, 5.87.

Carbonyl Sulfide, COS. A rapidly stirred hexane solution of **1** was allowed to react under an atmosphere of COS gas at 60 °C for 3 h to afford a yellow solution. The resultant complex was unreactive toward heating in a slow stream of nitrogen; i.e., the COS reaction was irreversible. IR (hexane): ν(CO) 2121 (w), 2086 (ms), 2081 (w), 2071 (w), 2065 (s), 2058 (vw), 2056 (vs), 2038 (w), 2024 (sh), 2016 (sh), 2013 (s), 2008 (sh), 1991 (m), and 1980 (vw) cm^{-1}.

Other Bases. Various Lewis bases were dissolved in hexane, the solutions were added dropwise to hexane solutions of **1**, and the reactions were monitored by infrared spectroscopy in the ν(CO) region.

(a) THF. New infrared bands were observed at 2103 (w), 2090 (w), 2069 (w), 2018 (vs), 1989 (w), 1943 (w), and 1931 (w) cm^{-1}. An insoluble product formed upon prolonged reaction.

(b) MeOH. New infrared bands were observed at 2104 (w), 2091 (vw), 2069 (m), 2055 (m), 2052 (m), 2038 (m), 2021 (s), 2000 (vw), 1989 (w), 1949 (w), 1943 (vw) cm^{-1}. An insoluble product formed upon further reaction.

(c) CH_3CN. New infrared bands were observed at 2097 (w), 2078 (m), 2032 (sh), 2017 (vs, br), 1993 (vw), 1948 (vw), and 1941 (m) cm^{-1}. The reaction was reversed upon removal of CH_3CN by evaporation.

(d) H_2O. This reaction was carried out between **1** and H_2O in either acetone or ether solutions. New infrared bands were observed: in acetone, 2085 (vw, br), 2047 (s, br), 2010 (vs, br), 1974 (w, sh), 1929 (w, br); in ether: 2089 (w, br), 2055 (s, br), 2013 (vs, br), 1992 (sh), 1935 (w, br). An insoluble product formed on further reaction.

(e) HNC_5H_{10} (Piperidine). New IR peaks were observed which grow in sequentially to indicate at least three new species. **8**: 2101 (m), 2038 (vw), 2031 (s), 2018 (vs), 1990 (w), 1943 (m) cm^{-1}. **9**: 2091 (mw), 2016 (vs), 1976 (ms), 1937 (m), 1925 (w) cm^{-1}. **10**: 2072 (m), 2007 (vs), 1982 (s), 1951 (vw), 1930 (mw) cm^{-1}. After several days, white needles (**11**) separated out of solution; these exhibited no ν(CO) vibrations but displayed bands in the O–H(phenolic), C–H(aromatic), and C–H(aliphatic) region of the infrared spectrum. ^1H NMR ($CDCl_3$) of **11**: δ(aromatic) H-2 7.29 (doublet of doublet), H-4 7.09 (doublet of triplet), H-5 6.92 (doublet of doublet), H-3 6.75 (doublet of triplet) (J_{ortho} = 8, J_{meta} = 1.6 Hz); δ(O–H phenolic) 7.09 (singlet); δ(aliphatic, piperidine group) 2.94 (singlet, broad, α to N), 1.56 (singlet, broad). Relative areas: aromatic:piperidine:OH: ca 8:10:2. Anal. Calc for $C_{17}NCl_2O_2H_{21}$: C, 59.60; H, 6.10; N, 4.09. Found: C, 59.42; H, 6.26; N, 4.08.

(f) No apparent reaction was observed between **1** and CO_2, ethylene, or H_2 as monitored by high pressure (600 psi) FTIR.

Synthesis of $Ru_3(CO)_8(\mu\text{-}\eta^2\text{-}OCH_2C_5H_4N)_2$ (12). The synthesis of the triruthenium derivative was carried out using $Ru_3(CO)_{12}$ (0.10 g, 0.16 mmol), anhydrous $(CH_3)_3NO$ (0.05 g, 0.70 mmol), and 0.10 mL of pyridinecarbinol in CH_2Cl_2 solution in a manner completely analogous to that employed in the preparation of **1**. The resultant bright yellow solution was filtered, and the filtrate was reduced in volume to 30 mL. Upon cooling, light yellow crystal of **12** were obtained in 55% yield. The infrared ν(CO) spectrum in CH_2Cl_2 displayed bands at 2073 (m), 1996 (vs), and 1919 (m) cm^{-1}. The ^1H NMR ($CDCl_3$) of the $-OCH_2C_5H_4N$ ligands follows. Aromatic region: H-1 δ 8.75, 8.73 (doublet, broadened) (J_{12} = 5.2 Hz); H-3 δ 7.56, 7.55; δ 7.52, 7.51; δ 7.48, 7.47 (doublet of triplets) ($J_{32} = J_{34}$ = 7.3 Hz); H-2 δ 7.23, 7.22, 7.19 (triplet under solvent peak); H-4 δ 6.56, 6.19 (doublet) (J_{34} = 7.3 Hz). Aliphatic region $H_{a/b}$: δ 5.08, 4.99 (doublet); δ 4.13, 4.04 (doublet) (J_{ab} = 18 Hz). Integrated area of aromatic signals to aliphatic signals = 4:2.

X-ray Structural Determinations of 1 and 12. An orange needle (0.30 mm × 0.40 mm × 0.60 mm) for **1** and an orange parallelepiped (0.14 mm × 0.36 mm × 0.38 mm) for **12** were mounted on a glass fiber with epoxy cement at room temperature and cooled to 193 K in a N_2 cold stream. Preliminary examination and data collection were performed on a Nicolet R3m/V X-ray diffractometer (oriented graphite monochromator; Mo Kα λ = 0.710 73 Å radiation). Cell parameters were calculated from the least-squares fitting of the setting angles for 25 reflections. ω scans for several intense reflections indicated acceptable crystal quality.

Data were collected for 4.0° ≤ 2θ ≤ 50.0° at 193 K. Scan ranges for the data collection were 1.60° plus Kα separation for **1** and 1.00° plus

(9) (a) The chemical shifts and coupling constants were calculated using an NMR simulation program for the IBM/PC and calculated chemical shift frequencies to ±1 Hz of observed frequencies. The assignments of chemical shifts for the hydrogens in the o-OC_6H_4Cl ligand were done using as criteria additive effects for the O and Cl atoms on the benzene ring. Expected values (ppm): H-1 (ortho to O), 6.75; H-2, 7.05–7.25; H-3, 6.9–6.75; H-4, 7.05–7.25 (Silverstein, R. M.; Bassler, G. C.; Morrill, J. C. *Spectrometric Identification of Organic Compounds*; 5th ed., John Wiley & Sons: New York, 1991. (b) Expected values (ppm) for o-chlorophenol ligand: C-1, 155.8; C-2, 122; C-3, 130.3; C-4, 124.3; C-5, 128; C-6, 117.1. Additive values taken from: Silverstein et al. in ref 9a.

Table 1. Crystallographic Data and Collection Parameters for **1** and **12**

formula	$C_{20}H_8O_{10}Cl_2Ru_3$	$C_{20}H_{12}N_2O_{10}Ru_3$
fw	782.4	743.5
space group	orthorhombic *Pbca*	monoclinic $P2_1/c$
a, Å	18.676(4)	12.305(3)
b, Å	9.106(2)	10.331(2)
c, Å	28.496(6)	18.489(4)
β, deg		90.67(2)
V, Å^3	4846(2)	2350.2(9)
Z	8	4
d(calcd), g/cm^3	2.145	2.101
abs coeff, mm^{-1}	2.086	1.924
λ, Å	0.710 73	0.710 73
T, K	193	296
transm coeff	0.7010/1.0000	0.7015/1.0000
R,[a] %	5.07	3.08
R_w,[a] %	7.50	4.16

[a] $R = \Sigma||F_o| - |F_c||/\Sigma F_o$. $R_w = \{[\Sigma w(F_o - F_c)^2]/[\Sigma w(F_o)^2]\}^{1/2}$.

Kα separation for **12**, with variable scan rates of 1.50–14.65° min^{-1} for **1** and 3.97–14.65° min^{-1} for **12**. Three control reflections, collected every 97 reflections, showed no significant trends. Background measurement was made by the stationary-crystal and stationary-counter technique at the beginning and end of each scan for half of the total scan time.

Lorentz and polarization corrections were applied to 4742 reflections for **1** and 8550 reflections for **12**. A semiempirical absorption correction was applied (thin-plate approximation; face (100); T_{max} = 1.0000, T_{min} = 0.7010 for **1** and ellipsoid approximation; μr = 0.05; T_{max} = 1.0000, T_{min} = 0.7015 for **12**). Totals of 3605 unique reflections for **1** and 3344 for **12**, with $|I| \geq 2.0\sigma I$, were used in further calculations. Both structures were solved by direct methods [SHELXS, SHELXTL-PLUS program package, Sheldrick (1988)]. Full-matrix least-squares anisotropic refinement for all non-hydrogen atoms [number of least-squares parameters = 316 for **1** and **12**; quantity minimized $\Sigma w(F_o - F_c)^2$; $w^{-1} = \sigma_F^2 + gF^2$, g = 0.001 00 for **1** and g = 0.000 10 for **12**] yielded R = 0.051, R_w = 0.075, and S = 2.03 for **1** and R = 0.031, R_w = 0.029, and S = 1.35 for **12** at convergence. Hydrogen atoms were placed in idealized positions with isotropic thermal parameters fixed at 0.08 Å. Neutral-atom scattering factors and anomalous scattering correction terms were taken from ref 10. Crystal data and experimental conditions are provided in Table 1.

Results and Discussion

Synthesis and Spectroscopic Characterization of 1 and Related Derivatives. The halide-stabilized triruthenium clusters were synthesized from $Ru_3(CO)_{12}$ and the appropriately substituted phenol, where CO loss was accomplished *via* oxidation to CO_2 under mild conditions using *anhydrous* Me_3NO. This procedure is analogous to that utilized in the preparation of the previously reported guaiacol (*o*-$MeOC_6H_4OH$) derivative.[7] It is important to note here that in the absence of a weak base substituent *ortho* to the oxygen atom in the phenolate ligand, the complexes are quite unstable. For example, when the reaction is carried out with phenol, presumably the initially formed complex, $Ru_3(CO)_{10}(\mu\text{-}OC_6H_5)_2$, is unstable with respect to further CO dissociation. Consistent with this observation, complex **1** reversibly reacts with carbon monoxide (vide infra). The ν(CO) infrared spectra of these complexes (typified in Figure 1a for the chloro derivative) displayed only terminal ν(CO) vibrations. Upon addition of carbon monoxide, the spectra became more complex, changing to that illustrated in Figure 1b for **1**, which subsequent to the removal of the CO atmosphere reverts to the original spectrum (Figure 1c).

The ^{1}H NMR spectra of the new compounds, recorded at ambient temperature, exhibited an ABCD pattern for the *o*-OC_6H_4X ligand (see simulated and observed spectra for **1** in Figure 2).[8] In addition, the absence of a hydride ligand in the complex is sustained by the lack of a Ru–*H* resonance in the ^{1}H NMR. The ambient-temperature ^{13}C NMR spectrum of complex **1** displayed five distinct peaks for the carbon atoms for the *o*-OC_6H_4Cl ligand at 159.9 (C-1), 119.4 (C-2 and C-6), 126.2

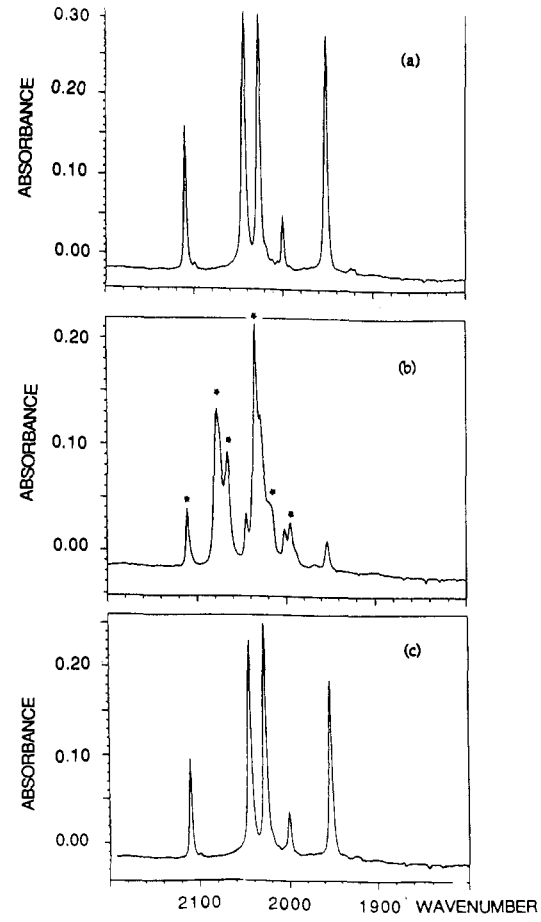

Figure 1. Infrared spectra in ν(CO) region of complex **1** in hexane solution: (a) pure complex in solution; (b) complex in the presence of an atmosphere of carbon monoxide (peaks marked by asterisks are new absorptions); (c) complex after removal of CO atmosphere.

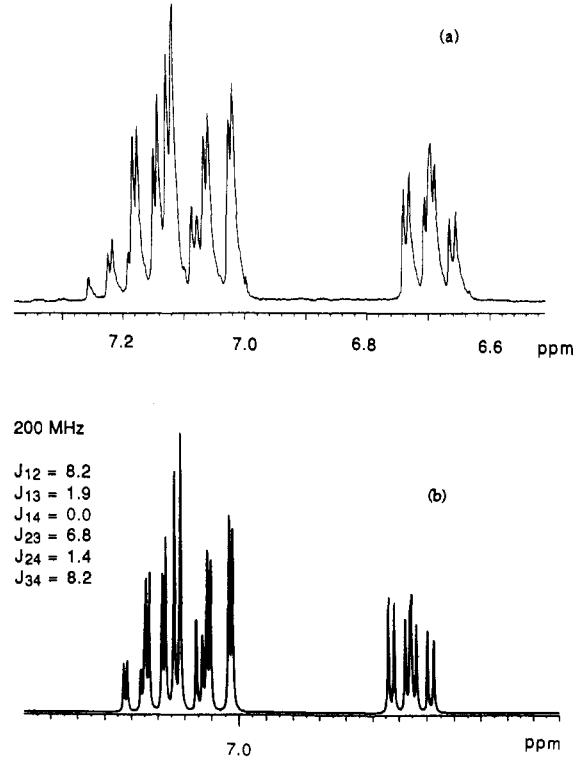

Figure 2. ^{1}H NMR spectra of $Ru_3(CO)_8(\mu\text{-}\eta^2\text{-}OC_6H_4Cl)_2$ (**1**) in $CDCl_3$: (a) observed; (b) simulated.

(10) *International Tables for X-Ray Crystallography*; Ibers, J. A., Hamilton, W. C., Eds.; Kynoch Press: Birmingham, England, 1974; Vol. IV, pp 99, 149.

Table 2. Atomic Coordinates (×10⁴) and Equivalent Isotropic Displacement Parameters (Å² × 10³) for Complex **1**[a]

	x	y	z	U(eq)[b]
Ru(1)	9296(1)	370(1)	3755(1)	21(1)
Ru(2)	10746(1)	-20(1)	3746(1)	25(1)
Ru(3)	10013(1)	-2627(1)	3786(1)	20(1)
Cl(2)	8977(1)	-4502(2)	3664(1)	29(1)
O(10)	9312(2)	-1381(5)	4240(1)	20(1)
O(3)	10703(3)	-374(6)	4819(2)	39(2)
O(4)	10479(3)	-45(7)	2670(2)	49(2)
O(7)	10933(3)	-3930(7)	4541(2)	50(2)
O(8)	11068(3)	-3827(6)	3094(2)	55(2)
C(8)	10651(3)	-3392(8)	3354(3)	31(2)
C(7)	10580(4)	-3432(8)	4252(2)	31(2)
C(3)	10707(3)	-234(8)	4423(3)	28(2)
C(13)	8715(3)	-1855(6)	4460(2)	20(2)
C(6)	9307(4)	1739(8)	3273(2)	35(2)
C(4)	10586(4)	-62(8)	3062(3)	37(2)
Cl(1)	7962(1)	-56(2)	3881(1)	33(1)
O(9)	9345(2)	-1544(5)	3308(1)	23(1)
O(6)	9305(4)	2535(7)	2967(2)	65(2)
C(11)	7792(3)	-3676(7)	2520(2)	33(2)
C(17)	7427(4)	-1673(8)	4588(2)	34(2)
C(8)	8836(3)	-2239(6)	3063(2)	22(2)
C(16)	7477(4)	-2670(8)	4948(3)	40(2)
C(10)	8084(3)	-4372(7)	2914(2)	27(2)
C(14)	8755(3)	-2851(7)	4829(2)	27(2)
C(15)	8140(4)	-3263(7)	5068(2)	36(2)
C(9)	8591(3)	-3637(6)	3175(2)	24(2)
C(12)	8034(3)	-1303(6)	4352(2)	23(2)
C(7)	8543(3)	-1573(7)	2660(2)	29(2)
C(6)	8041(4)	-2299(8)	2392(2)	35(2)
O(5)	9497(3)	2887(5)	4415(2)	43(2)
O(2)	11077(4)	3286(7)	3748(2)	62(2)
C(2)	10984(4)	2050(8)	3752(2)	29(2)
O(1)	12281(3)	-1223(12)	3716(2)	90(4)
C(5)	9401(3)	1904(7)	4169(2)	26(2)
C(1)	11710(4)	-788(11)	3723(3)	45(3)

[a] Estimated standard deviations are given in parentheses. [b] Equivalent isotropic U defined as one-third of the trace of the orthogonalized U_{ij} tensor.

Table 3. Selected Bond Lengths (Å)[a] for Complex **1**

Ru(1)–Ru(2)	2.732(1)	Ru(1)–Ru(3)	3.042(1)
Ru(1)–O(10)	2.110(4)	Ru(1)–C(6)	1.855(7)
Ru(1)–Cl(1)	2.547(2)	Ru(1)–O(9)	2.161(4)
Ru(1)–C(5)	1.839(6)	Ru(2)–Ru(3)	2.743(1)
Ru(2)–C(3)	1.940(7)	Ru(2)–C(4)	1.972(8)
Ru(2)–C(2)	1.936(7)	Ru(2)–C(1)	1.932(8)
Ru(3)–Cl(2)	2.604(2)	Ru(3)–O(10)	2.163(4)
Ru(3)–C(8)	1.848(7)	Ru(3)–C(7)	1.849(7)
Ru(3)–O(9)	2.093(4)	Cl(2)–C(9)	1.756(6)
O(10)–C(13)	1.350(7)	Cl(1)–C(12)	1.765(6)
O(9)–C(8)	1.338(7)		

[a] Estimated standard deviations are given in parentheses.

(C-3), 122.1 (C-4), and 127.9 ppm (C-5) along with two resonances due to Ru–*C*O at 197.4 and 184.4 ppm (vide infra).

Crystal Structure of $Ru_3(CO)_8(\mu\text{-}\eta^2\text{-}OC_6H_4Cl)_2$ (1). On the basis of infrared spectral similarities in the ν(CO) region of the spectra, complex **1** is thought to be prototypical of complexes derived from the reaction of $Ru_3(CO)_{12}$ and various substituted phenols. Hence, it was chosen for X-ray structural determination. The final atomic positional and equivalent isotropic displacement parameters are listed in Table 2. Selected interatomic distances and angles are given in Tables 3 and 4. An ORTEP view of the entire molecular unit is depicted in Figure 3, which also defines the atomic labeling scheme.

The two o-OC_6H_4Cl ligands are each coordinated to the same two ruthenium atoms (Ru(1) and Ru(3)) on the same side of the triangular cluster via μ-O atoms which behave as five-electron donors (see skeletal drawing in Figure 3). There is a slight asymmetry to the Ru–μ-O bonding, with Ru(1)–O(10) and Ru(3)–O(9) bond distances (average 2.10[4] Å) being shorter than the corresponding distances for the Ru(1)–O(9) and Ru(3)–O(10) (average 2.162[4] Å). Nevertheless, these Ru–μ-O distances, which average 2.132[4] Å, are quite similar to those found in the analogous guaiacol derivative (2.125 Å),[7] as well as those distances determined for the related triply bridged $[Ru_2(C_6H_6)_2(\mu\text{-}OMe)_3]^+$ ion (2.085 Å) and the $Os_3(CO)_{10}(\mu\text{-}OMe)_2$ derivative (2.085 Å).[11,12] The Ru(1)–Ru(3) distance is significantly longer (3.042(1) Å) than the other two ruthenium–ruthenium bonding distances of 2.732(1) and 2.743(1) Å, supporting a lack of metal–metal interaction in the former case. Each chloride group is coordinated to one of the two ruthenium centers which are μ-oxygen-bridged at an average distance of 2.576[2] Å, approximately trans to the unsupported Ru–Ru bonds. Two terminal carbonyls complete the coordination sphere of the two equivalent Ru atoms. The unique Ru atom has a $Ru(CO)_4$ structure similar to that of the parent carbonyl compound. The bidentate chelate μ-oxo nature of the o-OC_6H_4Cl ligand is similar to that reported for o-OC_6H_4OMe,[7] indicating the unusual C–Cl–Ru bridging Lewis base behavior toward Ru shown by the Cl atom. It is presumed that the same bonding arrangement is present for the F and Br in the analogous phenols and Cl in 2,6-dichlorophenol in the other compounds prepared.

Table 4. Selected Bond Angles (deg)[a] for Complex **1**

Ru(2)–Ru(1)–Ru(3)	56.4(1)	Ru(2)–Ru(1)–O(10)	83.9(1)
Ru(3)–Ru(1)–O(10)	45.3(1)	Ru(2)–Ru(1)–C(6)	94.0(2)
Ru(3)–Ru(1)–C(6)	128.3(2)	O(10)–Ru(1)–C(6)	173.0(2)
Ru(2)–Ru(1)–Cl(1)	162.1(1)	Ru(3)–Ru(1)–Cl(1)	106.9(1)
O(10)–Ru(1)–Cl(1)	78.9(1)	C(6)–Ru(1)–Cl(1)	102.5(2)
Ru(2)–Ru(1)–O(9)	81.2(1)	Ru(3)–Ru(1)–O(9)	43.5(1)
O(10)–Ru(1)–O(9)	77.1(2)	C(6)–Ru(1)–O(9)	96.0(2)
Cl(1)–Ru(1)–O(9)	90.1(1)	Ru(2)–Ru(1)–C(5)	89.9(2)
Ru(3)–Ru(1)–C(5)	128.0(2)	O(10)–Ru(1)–C(5)	98.8(2)
C(6)–Ru(1)–C(5)	87.9(3)	Cl(1)–Ru(1)–C(5)	97.5(2)
O(9)–Ru(1)–C(5)	170.5(2)	Ru(1)–Ru(2)–Ru(3)	67.5(1)
Ru(1)–Ru(2)–C(3)	88.1(2)	Ru(3)–Ru(2)–C(3)	81.6(2)
Ru(1)–Ru(2)–C(4)	82.0(2)	Ru(3)–Ru(2)–C(4)	87.0(2)
C(3)–Ru(2)–C(4)	167.1(3)	Ru(1)–Ru(2)–C(2)	95.8(2)
Ru(3)–Ru(2)–C(2)	163.1(2)	C(3)–Ru(2)–C(2)	95.6(3)
C(4)–Ru(2)–C(2)	93.6(3)	Ru(1)–Ru(2)–C(1)	166.2(3)
Ru(3)–Ru(2)–C(1)	98.8(3)	C(3)–Ru(2)–C(1)	91.8(3)
C(4)–Ru(2)–C(1)	95.8(3)	C(2)–Ru(2)–C(1)	98.0(3)
Ru(1)–Ru(3)–Ru(2)	56.1(1)	Ru(1)–Ru(3)–Cl(2)	104.9(1)
Ru(2)–Ru(3)–Cl(2)	158.9(1)	Ru(1)–Ru(3)–O(10)	43.9(1)
Ru(2)–Ru(3)–O(10)	82.7(1)	Cl(2)–Ru(3)–O(10)	88.5(1)
Ru(1)–Ru(3)–C(8)	127.1(2)	Ru(2)–Ru(3)–C(8)	88.7(2)
Cl(2)–Ru(3)–C(8)	98.2(2)	O(10)–Ru(3)–C(8)	170.4(2)
Ru(1)–Ru(3)–C(7)	128.9(2)	Ru(2)–Ru(3)–C(7)	95.0(2)
Cl(2)–Ru(3)–C(7)	105.1(2)	O(10)–Ru(3)–C(7)	97.1(2)
C(8)–Ru(3)–C(7)	87.7(3)	Ru(1)–Ru(3)–O(9)	45.3(1)
Ru(2)–Ru(3)–O(9)	82.1(1)	Cl(2)–Ru(3)–O(9)	77.2(1)
O(10)–Ru(3)–O(9)	77.4(2)	C(8)–Ru(3)–O(9)	97.4(2)
C(7)–Ru(3)–O(9)	174.0(2)	Ru(3)–Cl(2)–C(9)	96.7(2)
Ru(1)–O(10)–Ru(3)	90.8(2)	Ru(1)–O(10)–C(13)	122.3(3)
Ru(3)–O(10)–C(13)	127.6(4)	Ru(3)–C(8)–O(8)	177.1(6)
Ru(3)–C(7)–O(7)	179.8(7)	Ru(2)–C(3)–O(3)	178.1(5)
O(10)–C(13)–C(14)	121.1(5)	O(10)–C(13)–C(12)	122.2(5)
C(14)–C(13)–C(12)	116.6(5)	Ru(1)–C(6)–O(6)	177.4(6)
Ru(2)–C(4)–O(4)	177.7(6)	Ru(1)–Cl(1)–C(12)	97.5(2)
Ru(1)–O(9)–Ru(3)	91.3(2)	Ru(1)–O(9)–C(8)	131.2(4)
Ru(3)–O(9)–C(8)	122.7(4)		

[a] Estimated standard deviations are given in parentheses.

Crystal Structure of $Ru_3(CO)_8(\mu\text{-}\eta^2\text{-}OCH_2C_5H_4N)_2$ (12). Complex **12** was prepared from $Ru_3(CO)_{12}$ and 2 equiv of pyridinecarbinol via a process completely analogous to that described for the preparation of complex **1**. Crystals suitable for X-ray crystallography were obtained from a cooled dichloromethane solution. The final atomic positional and equivalent isotropic displacement parameters for complex **12** are listed in Table 5. Figure 4 illustrates an ORTEP drawing of the molecule, and selected bond distances and angles are provided in Tables 6 and 7.

(11) Gould, R. O.; Stephenson, T. A.; Tocher, D. A. *J. Organomet. Chem.* **1984**, *263*, 375.
(12) Allen, V. R.; Mason, R.; Hitchcock, P. B. *J. Organomet. Chem.* **1977**, *140*, 297.

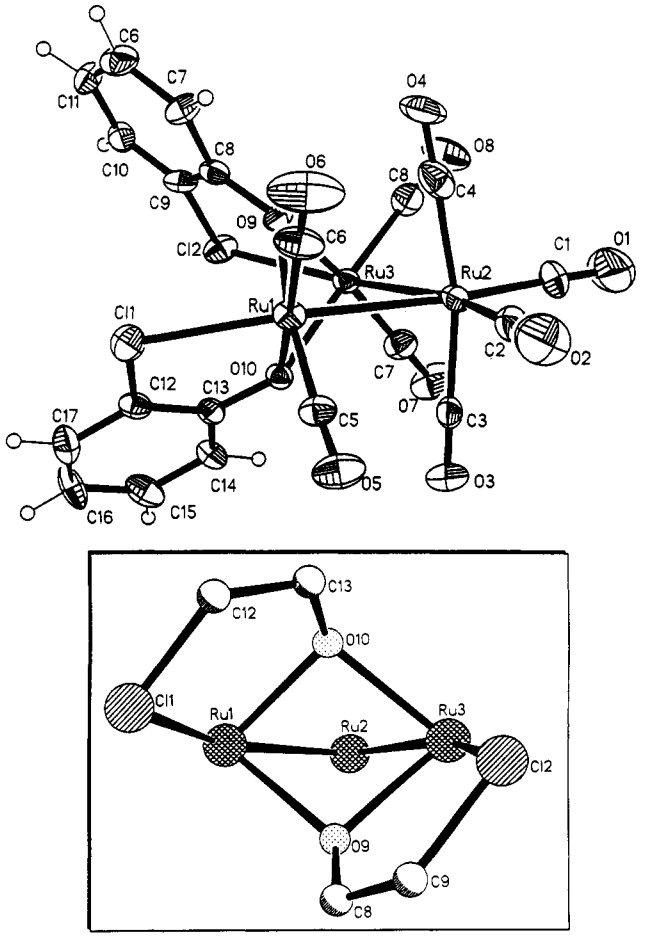

Figure 3. ORTEP drawing of **1** showing the atom-numbering scheme. Thermal elipsoids are drawn at the 50% probability level. The boxed view illustrates the μ-η^2-OC_6H_4Cl binding to the Ru(1)···Ru(3) unit.

Analogous to the arrangement of aryloxide ligands in complex **1**, the two $-OCH_2C_5H_4N$ groups are each bonded to the same two ruthenium atoms (Ru(2) and Ru(3)) of the triangular cluster by way of the alkoxide's μ-O atoms, which behave as three-electron donors. These bridging alkoxide ligands display a slight asymmetry in their binding to the two ruthenium centers, with the Ru(3)–O(10) and Ru(2)–O(10) distances at 2.080(3) and 2.152(3) Å being complemented by Ru(3)–O(9) and Ru(2)–O(9) distances of 2.166(3) and 2.109(3) Å. The Ru–Ru edge which bears the μ-O bridges (Ru(2)···Ru(3)) at 3.024(1) Å is significantly longer than the other two bonding Ru–Ru distances (Ru(1)–Ru(2) = 2.786(1) Å and Ru(1)–Ru(3) = 2.779(1) Å). Each pyridine substituent is bonded to one of the two ruthenium atoms which are μ-oxygen-bridged at an average distance of 2.160[4] Å; i.e., Ru(3)–N(2) = 2.164(3) and Ru(2)–N(1) = 2.155(4) Å. The coordination sphere of each of the two equivalent ruthenium atoms is completed by two carbonyl ligands, whereas the unique ruthenium center has a $Ru(CO)_4$ geometry similar to that seen in the parent triruthenium dodecacarbonyl cluster.

Reactivity Studies of Complex 1. The observation of a reversible addition of CO to complex **1** suggested a more detailed investigation of this system by FTIR and ^{13}C VT NMR spectroscopies. In addition, an extension of these studies to include Lewis bases other than carbon monoxide is warranted.

The variable-temperature ^{13}C NMR spectra for the highly ^{13}CO-enriched complex (**1a**) in $CDCl_3$ over the temperature range +23 to −60 °C are shown in Figure 5. The ambient-temperature spectrum exhibits, in the Ru–*C*O region, two sharp singlets at 198.4 and 185.3 ppm and a broad peak centered at 200.4 ppm. At 0 °C, the peak at 200.4 ppm has broadened considerably, with coalescence occurring around −5 °C. When the temperature was further lowered to −10 °C, two peaks began to emerge at

Table 5. Atomic Coordinates (×10⁴) and Equivalent Isotropic Displacement Parameters (Å³ × 10³) for Complex **12**[a]

	x	*y*	*z*	*U*(eq)[b]
Ru(1)	8369(1)	3728(1)	1389(1)	37(1)
Ru(2)	7735(1)	1638(1)	529(1)	34(1)
Ru(3)	7572(1)	1629(1)	2160(1)	31(1)
O(1)	8836(4)	5071(4)	2835(2)	90(2)
O(2)	10602(3)	2387(4)	1355(2)	74(2)
O(3)	5978(3)	4523(3)	1227(2)	61(1)
O(4)	8982(3)	5741(4)	245(3)	96(2)
O(5)	9378(3)	1831(4)	3247(2)	78(2)
O(6)	6271(3)	3405(3)	3089(2)	67(1)
O(7)	9777(3)	1549(4)	−328(2)	82(2)
O(8)	6775(3)	3530(4)	−524(2)	72(2)
O(9)	6434(2)	1532(3)	1259(1)	33(1)
O(10)	8447(2)	561(3)	1412(1)	33(1)
N(1)	6988(3)	−162(3)	207(2)	39(1)
N(2)	7096(3)	−324(3)	2435(2)	34(1)
C(1)	8676(4)	4616(5)	2285(3)	56(2)
C(2)	9767(4)	2830(5)	1372(3)	49(2)
C(3)	6861(4)	4182(5)	1298(2)	42(2)
C(4)	8782(4)	4973(5)	671(3)	59(2)
C(5)	8683(4)	1770(4)	2835(3)	45(2)
C(6)	6750(4)	2693(5)	2741(2)	41(2)
C(7)	8993(4)	1608(5)	−9(3)	49(2)
C(8)	7133(4)	2790(5)	−124(3)	48(2)
C(9)	7402(4)	−1046(5)	−260(2)	47(2)
C(10)	6989(4)	−2279(5)	−322(3)	52(2)
C(11)	6113(4)	−2626(5)	88(3)	56(2)
C(12)	5674(4)	−1731(4)	556(3)	45(2)
C(13)	6128(3)	−506(4)	605(2)	33(1)
C(14)	5690(3)	514(4)	1109(2)	34(1)
C(15)	6323(3)	−695(5)	2902(2)	41(2)
C(16)	6009(4)	−1972(5)	2972(3)	50(2)
C(17)	6521(4)	−2897(5)	2564(3)	54(2)
C(18)	7315(4)	−2538(5)	2097(2)	49(2)
C(19)	7598(3)	−1237(4)	2038(2)	34(1)
C(20)	8484(3)	−785(4)	1545(2)	39(1)

[a] Estimated standard deviations are given in parentheses. [b] Equivalent isotropic *U* defined as one-third of the trace of the orthogonalized U_{ij} tensor.

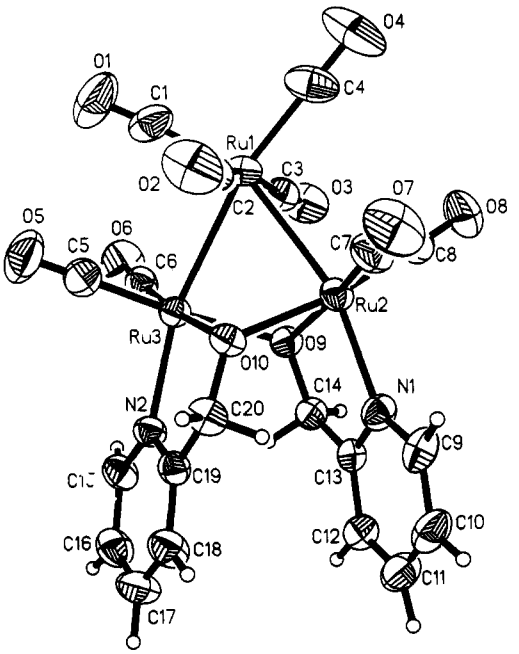

Figure 4. ORTEP drawing of **12** showing the atom-numbering scheme. Thermal elipsoids are drawn at the 50% probability level.

201.8 and 199.3 ppm which eventually became a pair of doublets at -40 °C. At −60 °C, the two doublets are clearly seen at 202.2 and 202.0 ppm and at 199.6 and 199.4 ppm, along with two singlets superimposed at the center of each doublet (202.1 and 199.5 ppm). Hence, the two doublets correspond to two types of carbonyl ligands coupled to one another ($J_{^{13}C-^{13}C}$ = 35 Hz) in

Table 6. Selected Bond Lengths (Å)[a] for Complex **12**[a]

Ru(1)–Ru(2)	2.786(1)	Ru(1)–Ru(3)	2.779(1)
Ru(1)–C(1)	1.928(6)	Ru(1)–C(2)	1.955(5)
Ru(1)–C(3)	1.919(5)	Ru(1)–C(4)	1.921(6)
Ru(2)–Ru(3)	3.024(1)	Ru(2)–O(9)	2.109(3)
Ru(2)–O(10)	2.152(3)	Ru(2)–N(1)	2.155(4)
Ru(2)–C(7)	1.850(5)	Ru(2)–C(8)	1.846(5)
Ru(3)–O(9)	2.166(3)	Ru(3)–O(10)	2.080(3)
Ru(3)–N(2)	2.164(3)	Ru(3)–C(5)	1.845(5)
Ru(3)–C(6)	1.847(4)	O(1)–C(1)	1.135(7)
O(2)–C(2)	1.126(6)	O(3)–C(3)	1.149(6)
O(4)–C(4)	1.148(7)	O(5)–C(5)	1.141(6)
O(6)–C(6)	1.145(6)	O(7)–C(7)	1.139(6)
O(8)–C(8)	1.148(6)	O(9)–C(14)	1.419(5)
O(10)–C(20)	1.413(5)	N(1)–C(9)	1.360(6)
N(1)–C(13)	1.343(5)	N(2)–C(15)	1.347(5)
N(2)–C(19)	1.348(5)	C(9)–C(10)	1.375(7)
C(10)–C(11)	1.374(7)	C(11)–C(12)	1.380(7)
C(12)–C(13)	1.385(6)	C(13)–C(14)	1.511(6)
C(15)–C(16)	1.382(7)	C(16)–C(17)	1.374(7)
C(17)–C(18)	1.363(7)	C(18)–C(19)	1.393(7)
C(19)–C(20)	1.504(6)		

[a] Estimated standard deviations are given in parentheses.

Table 7. Selected Bond Angles (deg)[a] for Complex **12**[a]

Ru(2)–Ru(1)–Ru(3)	65.8(1)	Ru(2)–Ru(1)–C(1)	155.5(2)
Ru(3)–Ru(1)–C(1)	89.8(2)	Ru(2)–Ru(1)–C(2)	82.2(1)
Ru(3)–Ru(1)–C(2)	87.3(1)	C(1)–Ru(1)–C(2)	94.3(2)
Ru(2)–Ru(1)–C(3)	82.9(1)	Ru(3)–Ru(1)–C(3)	83.6(1)
C(1)–Ru(1)–C(3)	97.9(2)	C(2)–Ru(1)–C(3)	164.7(2)
Ru(2)–Ru(1)–C(4)	101.5(2)	Ru(3)–Ru(1)–C(4)	167.0(2)
C(1)–Ru(1)–C(4)	103.0(2)	C(2)–Ru(1)–C(4)	93.8(2)
C(3)–Ru(1)–C(4)	92.3(2)	Ru(1)–Ru(2)–O(9)	83.4(1)
Ru(1)–Ru(2)–O(10)	81.9(1)	O(9)–Ru(2)–O(10)	78.1(1)
Ru(1)–Ru(2)–N(1)	160.3(1)	Ru(3)–Ru(2)–N(1)	103.9(1)
O(9)–Ru(2)–N(1)	78.9(1)	O(10)–Ru(2)–N(1)	86.1(1)
Ru(1)–Ru(2)–C(7)	95.1(1)	Ru(3)–Ru(2)–C(7)	127.0(1)
O(9)–Ru(2)–C(7)	171.7(2)	O(10)–Ru(2)–C(7)	93.6(2)
N(1)–Ru(2)–C(7)	101.2(2)	Ru(1)–Ru(2)–C(8)	88.9(2)
Ru(3)–Ru(2)–C(8)	128.6(2)	O(9)–Ru(2)–C(8)	98.7(2)
O(10)–Ru(2)–C(8)	170.6(2)	N(1)–Ru(2)–C(8)	102.0(2)
C(7)–Ru(2)–C(8)	89.5(2)	Ru(1)–Ru(3)–O(9)	82.6(1)
Ru(1)–Ru(3)–O(10)	83.4(1)	O(9)–Ru(3)–O(10)	78.4(1)
Ru(1)–Ru(3)–N(2)	161.1(1)	Ru(2)–Ru(3)–N(2)	105.0(1)
O(9)–Ru(3)–N(2)	87.9(1)	O(10)–Ru(3)–N(2)	78.8(1)
Ru(1)–Ru(3)–C(5)	91.3(1)	Ru(2)–Ru(3)–C(5)	128.1(2)
O(9)–Ru(3)–C(5)	172.2(2)	O(10)–Ru(3)–C(5)	96.1(2)
N(2)–Ru(3)–C(5)	96.6(2)	Ru(1)–Ru(3)–C(6)	91.9(1)
Ru(2)–Ru(3)–C(6)	128.4(1)	O(9)–Ru(3)–C(6)	96.9(2)
O(10)–Ru(3)–C(6)	173.7(2)	N(2)–Ru(3)–C(6)	105.5(2)
C(5)–Ru(3)–C(6)	88.1(2)	Ru(2)–O(9)–Ru(3)	90.0(1)
Ru(2)–O(9)–C(14)	113.9(2)	Ru(3)–O(9)–C(14)	126.5(2)
Ru(2)–O(10)–Ru(3)	91.2(1)	Ru(2)–O(10)–C(20)	130.8(2)
Ru(3)–O(10)–C(20)	115.0(2)	Ru(2)–N(1)–C(9)	126.4(3)
Ru(2)–N(1)–C(13)	114.4(3)	C(9)–N(1)–C(13)	118.2(4)
Ru(3)–N(2)–C(15)	127.6(3)	Ru(3)–N(2)–C(19)	113.4(3)
C(15)–N(2)–C(19)	118.8(4)	Ru(1)–C(1)–O(1)	175.7(5)
Ru(1)–C(2)–O(2)	175.6(4)	Ru(1)–C(3)–O(3)	175.9(4)
Ru(1)–C(4)–O(4)	176.8(4)	Ru(3)–C(5)–O(5)	178.4(4)
Ru(3)–C(6)–O(6)	176.5(4)	Ru(2)–C(7)–O(7)	177.6(4)
Ru(2)–C(8)–O(8)	178.3(5)		

[a] Estimated standard deviations are given in parentheses.

the highly ^{13}CO-enriched molecules and the two singlets correspond to partially enriched molecules. On the other hand, the two sharp singlets at 198.4 and 185.3 ppm remain unchanged when the temperature is lowered. Thus the molecule shows a fluxional set of carbonyls exhibiting extensive scrambling at room temperature, slowing down to two types of equivalent CO ligands at low temperature. The other two singlets which are temperature invariant indicate a set of two types of carbonyls rigid in the temperature range studied (−60 to +23 °C). The fluxional set of carbonyl ligands are assigned to the unique $Ru(CO)_4$ moiety, which is known to possess a low-energy barrier for axial/equatorial carbonyl exchange.[6c] The set of two rigid carbonyls correspond to the two pairs of terminal CO on the Ru atoms bridged by the o-OC_6H_4Cl ligand, which cannot easily exchange intramolecularly

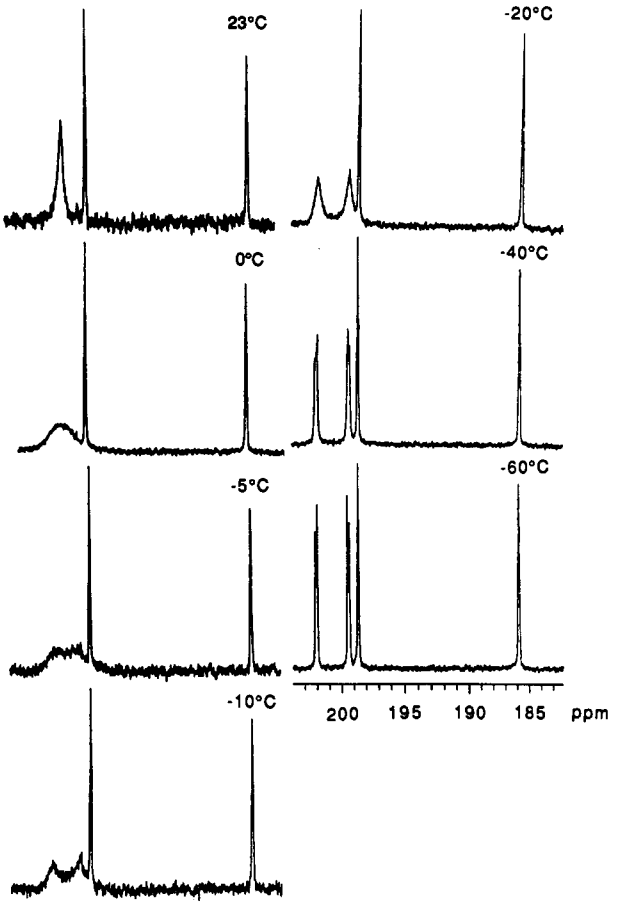

Figure 5. Variable-temperature ^{13}C NMR spectra of ^{13}CO-enriched **1** in $CDCl_3$.

due to the rigid bridging ligand present. This elucidation of the dynamic behavior of the ^{13}C NMR spectrum of complex **1** is consistent with that reported for the analogous dinitrosyl-bridged ruthenium cluster $Ru_3(CO)_{10}(NO)_2$. In this particular derivative, the $Ru(CO)_3$ units are rigid in the temperature range −50 to +40 °C, whereas the $Ru(CO)_4$ unit is stereochemically nonrigid *via* axial/equatorial exchange.[13,14]

Upon the addition of an atmosphere of carbon monoxide to a hexane solution of **1**, extra ν(CO) infrared bands appear at 2111, 2077, 2066, 2033, 2018, and 1995 cm^{-1} (see peaks marked by asterisks in Figure 1b). These supplementary ν(CO) bands are quickly lost with concomitant quantitative reappearance of the ν(CO) vibrations corresponding to **1** simultaneous with removal of the CO atmosphere (Figure 1c). When a ^{13}CO atmosphere is added to a hexane solution of complex **1** for a short period (<30 min at ambient temperature) and subsequently removed, the three lower frequency ν(CO) vibrations in Figure 1a (2027, 2001, and 1953 cm^{-1}) are readily replaced by peaks at 2018, 1963, and 1909 cm^{-1}. On the contrary, the higher frequency vibrations originally observed at 2111 and 2044 cm^{-1} are only slightly shifted by about 2 cm^{-1}. This behavior is reversible in that ^{12}CO can be added and then removed with the original spectrum being observed.

A logical interpretation of these infrared spectral changes is that the CO's primarily responsible for the three lower frequency bands correspond to the two $Ru(CO)_2$ units which are bridged by phenoxy ligands. These sites can undergo intermolecular exchange with free CO *via* CO displacement of the weakly bound chloride, thus providing an easy means for introducing labeled CO (Scheme 1). On the other hand, the carbonyl groups primarily responsible for the two higher frequency bands correspond to the

(13) Forster, A.; Johnson, B. F. G.; Lewis, J.; Matheson, T. W.; Robinson, B. H.; Jackson, W. G. *J. Chem. Soc., Chem. Commun.* **1974**, 1042.
(14) Bryan, E. G.; Forster, A.; Johnson, B. F. G.; Lewis, J.; Matheson, T. W. *J. Chem. Soc., Dalton Trans.* **1978**, 196.

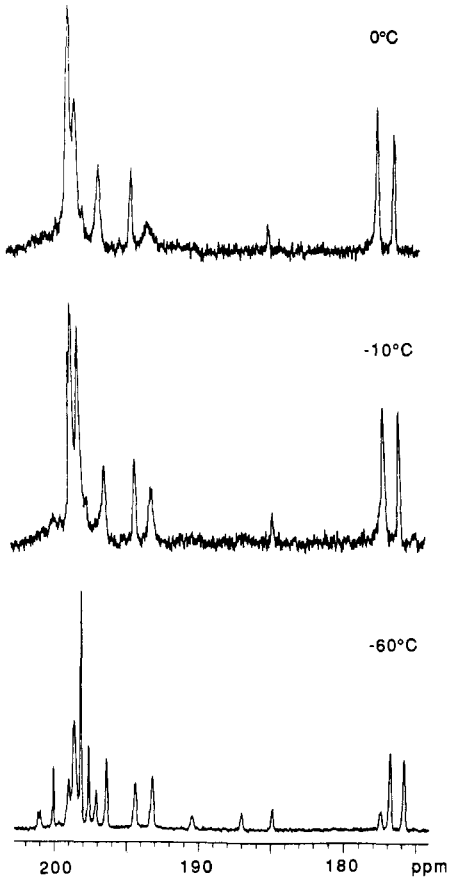

Figure 6. Variable-temperature ^{13}C NMR spectra of ^{13}CO-enriched **1** in an atmosphere of ^{13}CO in $CDCl_3$.

Scheme 1

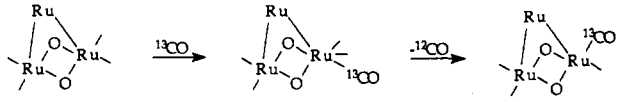

13

unique $Ru(CO)_4$ moiety which has no low-energy pathway for incorporating external labeled ^{13}CO as well as no low-energy barrier for exchanging with the other CO group as revealed by ^{13}C NMR studies.

The intermediacy of a $Ru_3(CO)_9$ species, **13**, in the CO exchange process is suggested on the basis of the variable-temperature ^{13}C NMR spectrum of complex **1** in the presence of an atmosphere of ^{13}CO in $CDCl_3$. That is, the spectrum can again be divided into two regions, a fluxional region due to $Ru(CO)_4$ and a more rigid region due to CO ligands attached to the ruthenium centers bridged by phenoxy ligands. This latter region of the limiting ^{13}C NMR spectrum contains five peaks of comparable intensity which are attributed to species **13**. In the ambient-temperature spectrum, one of these signals is undergoing exchange with free ^{13}CO in solution, a process slowed down considerably at −10 °C. Concomitantly, the $Ru(CO)_4$ region of the spectrum is complex, exhibiting resonances due to the parent complex (**1**), **13**, and its dicarbonyl-substituted derivative. The limiting spectrum in this region is afforded at about −60 °C (see Figure 6). The other small signals in the upfield region of the spectrum are assigned to the symmetrical $Ru_3(CO)_{10}(\mu\text{-}OC_6H_4Cl)_2$ derivative.

When strongly binding ligands such as pyridine or triphenylphosphine are added to complex **1**, sequential formations of $Ru_3(CO)_{10-n}(\mu\text{-}OC_6H_4Cl)_2L_n$ (n = 1, 2) derivatives are produced (**14**). In the instance of PPh_3, the initial complex which forms appears to be, on the basis of similarities in $\nu(CO)$ infrared spectra, the result of a simple substitution of the chloro substituent of phenol with PPh_3 as in **14**. However, further reaction affords

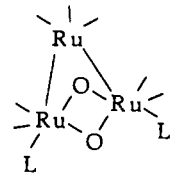

14

a product derived for C–H activation occurring with concomitant loss of the phenol ligands to provide the orthometalated derivative $Ru_3(CO)_8(C_6H_4PPh_2)_2$. The final product is the result of CO insertion into the metal–aryl bond. Nevertheless, a definitive structural assignment must await an X-ray crystallographic study of this triphenylphosphine-derived product. On the other hand, the solid-state structure determined for complex **12** is representive of the anticipated structure for species **14** when L = pyridine.

Concluding Remarks

The doubly bridged μ-OR triruthenium clusters presented herein are analogous, in both solid-state and solution structures, to the previously described dinitrosyl clusters $Ru_3(CO)_{10}(NO)_2$ and $Ru_3(CO)_8(PPh_3)_2(NO)_2$.[15] That is, in both instances the presence of two three-electron-donor groups impart two additional electrons to the cluster framework, resulting in metal–metal bond cleavage. For example, the doubly bridged nitrosyl and aryloxide/alkoxide Ru···Ru distances at 3.15 and 3.042/3.024 Å are considerably longer than the two nonbridged Ru–Ru edges and hence are considered to be nonbonding.

The facile displacement of carbonyl ligands in the initially formed $Ru_3(CO)_{10}(\mu\text{-}OC_6H_4X)_2$ derivatives is consistent with studies which demonstrate the interaction of anions with $Ru_3(CO)_{12}$ to be highly CO labilizing.[6,16–19] Similar behavior has also been noted in mononuclear metal carbonyl derivatives containing aryloxide or alkoxide ligands.[20,21] Indeed in the case of $Ru_3(CO)_{12}$ this property is generally regarded as being a precondition to catalytic activity, i.e., CO labilization provides the necessary open coordination site at the metal center.[19]

Acknowledgment. Financial support of this research by the Robert A. Welch Foundation is greatly appreciated. Professor B. Fontal is thankful to the Universidad de Los Andes for a sabbatical during which time this work was carried out.

Supplementary Material Available: Tables providing complete listings of bond lengths, bond angles, and anisotropic thermal parameters for complexes **1** and **12** (6 pages). Ordering information is given on any current masthead page.

(15) Norton, J.; Collman, J.; Dolcetti, G.; Robinson, W. T. *Inorg. Chem.* **1972**, *11*, 382.
(16) Fjare, J. L.; Jensen, J. A.; Gladfelter, W. L. *Inorg. Chem.* **1983**, *22*, 1774.
(17) Lavigne, G.; Kaesz, H. D. *J. Am. Chem. Soc.* **1984**, *106*, 4647.
(18) Lavigne, G.; Lugan, N.; Bonnet, J.-J. *Inorg. Chem.* **1987**, *26*, 2345.
(19) See also: Gladfelter, W. L.; Roesselet, K. J. In *The Chemistry of Metal Cluster Complexes*; Shriver, D. F., Kaesz, H. D., Adams, R. D., Eds.; VCH Publishers: New York, 1990; p 329.
(20) (a) Tooley, P. A.; Ovalles, C.; Kao, S. C.; Darensbourg, D. J.; Darensbourg, M. Y. *J. Am. Chem. Soc.* **1986**, *108*, 5465. (b) McNeese, T. J.; Mueller, T. E.; Wierda, D. A.; Darensbourg, D. J.; Delord, T. J. *Inorg. Chem.* **1985**, *24*, 3465. (c) McNeese, T. J.; Cohen, M. B.; Foxman, B. M. *Organometallics* **1984**, *3*, 552. (d) Darensbourg, D. J.; Sanchez, K. M.; Reibenspies, J. H.; Rheingold, A. L. *J. Am. Chem. Soc.* **1989**, *111*, 7094. (e) Darensbourg, D. J.; Mueller, B. L; Reibenspies, J. H.; Bischoff, C. J. *Inorg. Chem.* **1990**, *29*, 1789. (f) Darensbourg, D. J.; Mueller, B. L.; Bischoff, C. J.; Johnson, C. C.; Sanchez, K. M.; Reibenspies, J. H. *Isr. J. Chem.* **1990**, *30*, 369. (g) Darensbourg, D. J.; Mueller, B. L.; Bischoff, C. J.; Chojnacki, S. S.; Reibenspies, J. H. *Inorg. Chem.* **1991**, *30*, 2418.
(21) Lunder, D. M.; Lobkovsky, E. B.; Streib, W. E.; Caulton, K. G. *J. Am. Chem. Soc.* **1991**, *113*, 1837.